

# An investigation on dissolution kinetics of single sodium carbonate particle with image analysis method

Li, Changdong; Amador, Carlos; Ding, Yulong

DOI:

[10.1016/j.cjche.2016.08.001](https://doi.org/10.1016/j.cjche.2016.08.001)

License:

Creative Commons: Attribution-NonCommercial-NoDerivs (CC BY-NC-ND)

*Document Version*

Peer reviewed version

*Citation for published version (Harvard):*

Li, C, Amador, C & Ding, Y 2016, 'An investigation on dissolution kinetics of single sodium carbonate particle with image analysis method', *Chinese Journal of Chemical Engineering*.  
<https://doi.org/10.1016/j.cjche.2016.08.001>

[Link to publication on Research at Birmingham portal](#)

## General rights

Unless a licence is specified above, all rights (including copyright and moral rights) in this document are retained by the authors and/or the copyright holders. The express permission of the copyright holder must be obtained for any use of this material other than for purposes permitted by law.

- Users may freely distribute the URL that is used to identify this publication.
- Users may download and/or print one copy of the publication from the University of Birmingham research portal for the purpose of private study or non-commercial research.
- User may use extracts from the document in line with the concept of 'fair dealing' under the Copyright, Designs and Patents Act 1988 (?)
- Users may not further distribute the material nor use it for the purposes of commercial gain.

Where a licence is displayed above, please note the terms and conditions of the licence govern your use of this document.

When citing, please reference the published version.

## Take down policy

While the University of Birmingham exercises care and attention in making items available there are rare occasions when an item has been uploaded in error or has been deemed to be commercially or otherwise sensitive.

If you believe that this is the case for this document, please contact [UBIRA@lists.bham.ac.uk](mailto:UBIRA@lists.bham.ac.uk) providing details and we will remove access to the work immediately and investigate.

Accepted Manuscript

An Investigation on Dissolution Kinetics of Single Sodium Carbonate Particle with Image Analysis Method

Changdong Li, Carlos Amador, Yulong Ding

PII: S1004-9541(16)30752-2  
DOI: doi: [10.1016/j.cjche.2016.08.001](https://doi.org/10.1016/j.cjche.2016.08.001)  
Reference: CJCHE 634

To appear in:

Received date: 6 January 2016  
Revised date: 23 June 2016  
Accepted date: 27 July 2016



Please cite this article as: Changdong Li, Carlos Amador, Yulong Ding, An Investigation on Dissolution Kinetics of Single Sodium Carbonate Particle with Image Analysis Method, (2016), doi: [10.1016/j.cjche.2016.08.001](https://doi.org/10.1016/j.cjche.2016.08.001)

This is a PDF file of an unedited manuscript that has been accepted for publication. As a service to our customers we are providing this early version of the manuscript. The manuscript will undergo copyediting, typesetting, and review of the resulting proof before it is published in its final form. Please note that during the production process errors may be discovered which could affect the content, and all legal disclaimers that apply to the journal pertain.

**Materials and Product Engineering**

**Received 6 January 2016**

**Received in revised form 23 June 2016**

**Accepted 27 July 2016**

## **An investigation on dissolution kinetics of single sodium carbonate particle with image analysis method**

Changdong Li<sup>1</sup>, Carlos Amador<sup>2</sup> and Yulong Ding<sup>3\*</sup>

<sup>1</sup> *Institute of Particle Science and Engineering, University of Leeds, Leeds, UK*

<sup>2</sup> *Procter & Gamble Newcastle-Upon-Tyne Innovation Centre, Newcastle, UK*

<sup>3</sup> *School of Chemical Engineering, University of Birmingham, Birmingham, UK*

### **1. Introduction**

Dissolution of solid particles has been studied over one century and it is widely applied into various chemical and physical applications such as food industry, pharmaceutical and household product. A typical dissolution is generally the process of solute forming a solution in solvent. Three main dissolution models are thus developed including mass transport model, surface reaction model and inter-facial barrier model[1]. Based on these dissolution models[2], a vast number of mathematical models were proposed, such as Noyes-Whitney equation[3] and Hixson-Crowell model[4], and used to quantify the dissolution kinetics at different dissolving conditions.

Traditional dissolution studies mainly rely on the dissolution experiments such as U.S. Pharmacopeia (USP) dissolution apparatus[5]. The dissolution process usually is measured with conductivity or refractometry measurements. Dissolution mechanisms can be interpreted with the existing dissolution models. Although conventional research is normally based on the dissolution tests of bulk of particles, many dissolution studies with the approach of single particle have been raised and implemented into several materials in the recent 20 years. For example Dorozhkin quantified the dissolution kinetics of single crystal of natural fluorapatite with optical microscopy, SEM, Auger electron and IR reflection spectroscopy[6]. Raghavan et al. quantified the dissolution kinetics of single crystal of  $\alpha$ -lactose monohydrate, and linear dissolution profiles were determined as a function of time[7]. Štěpánek simulated the effective dissolution according to the local fluxes as the solution of a convection-diffusion problem in the surrounding liquid phase[8]. However, it is rarely investigated for sodium carbonate which is one of the most important basic compositions of many products such as detergent and baking powders with the approach of single particle to study the dissolution kinetics. The dissolution properties of sodium carbonate show a large extend to affect the quality of final products. Therefore, this work is highly motivated to overcome this vacancy of dissolution studies for sodium carbonate with the approach of single particle to determine its dissolution mechanism at different conditions and quantify its dissolution kinetics. The dissolution conditions that affect dissolution kinetics of solid particles generally based on the physical and chemical properties of

\* Corresponding author email: y.ding@bham.ac.uk

solution[9-10]. In this work, the dissolution experiments are carried out with increasing temperature and pH separately. Therefore, the dissolution mechanism of single sodium carbonate particle at increasing temperature and pH can be investigated and the dissolution kinetics are also quantified. In this way, the works in this paper will also provide vast information to extend the understanding of dissolution properties of sodium carbonate from the approach of single particle to bulk.

The dissolution process of single particle is normally excessively fast and the entire dissolution environment changes within a very small scale, it therefore is very difficult to measure the dissolution process directly with the measurement techniques which are usually applied for a bulk of particles. To accomplish the dissolution experiments of single sodium carbonate particle in this work, the image analysis method via high speed camera is implemented. Different with image analysis with microscopy, high speed camera has its great advances to transfer the entire dissolution process into visualized videos and each frame of video can be saved into dissolution images for analysis. The time scale of saved images can be accurate to 1/10, 1/20 or 1/50 second. In this way, it is reliable to apply image analysis method accurately into quantification of dissolution process of single sodium carbonate particle.

## **2. Sample selection**

The original sodium carbonate particles used in this work are provided by Procter & Gamble Newcastle Innovation Center (UK). The purity of sodium carbonate particles is 99.9%. The samples of sodium carbonate particle used into dissolution experiments are selected with the following procedures: firstly, the original sodium carbonate particles provided by Procter & Gamble are weighed for one particle by another in order to select the particles containing the mass of  $0.30 \pm 0.02$  mg. Then the selected particles from with same mass are observed with an optical microscopy to define their shape and only the particles having the shape of sphere are selected. The definition of particle shape in this work is based on the classification scheme by Riley[11]. According to Riley's definition, the particles having the sphericity higher than 0.775 can be considered as the high spherical particles where the sphericity is measured as the ratio of the diameter of a circle having the same area of measured particle to the diameter of the smallest circumscribed circle of measured particles. In this way, the optical microscopy of Nikon Eclipse Ti Microscopy is used in this step to measure the sphericity and the particles with the sphericity higher than 0.775 are selected as the spherical sodium carbonate particles. Finally, the diameter of spherical sodium carbonate particles is measured with this optical microscopy. Only the spherical particles having  $1.50 \pm 0.02$  mm diameter which is measured from its smallest circumscribed circle are selected as the samples used into the dissolution experiments. An example of the sample of spherical sodium carbonate particle was shown in Fig.1.

## **3. Experimental methodology**

The scheme of a typical dissolution experiment in this work is shown in Fig.2. For a typical dissolution experiment, one sample of spherical sodium carbonate particle is placed at the bottom of a transparent 12mm square glass cell. The transparent 12mm square glass cell used in this work is 12mm Glass Cell (PCS115) purchased from Malvern Tec. The high speed camera of Photron Fastcam SA5 is set-up with the frame of 50 FPS and resolution of 640x640 to record the dissolution process of this sample. When the high speed camera

starts to record, the cell is immediately filled with 0.2ml solution. In this way, the dissolution process of the sample is recorded as a video and the video also is transferred into 50 images per second automatically. These images are then used to measure the diameter of particle with dissolution time. Because the density of sodium carbonate particles used in this work is assumed to be a constant, the concentration of dissolved sodium carbonate is calculated based on the measured diameter values. In this way, the dissolution rate constant is thus quantified based on the calculated concentration of sodium carbonate by fitting with the mathematical model for each case.

The solvent used in dissolution experiments is deionized water and it is prepared in advance to obtain required temperature and pH. To obtain different temperature, the deionized water is pre-heated to 30°C, 40°C, 50°C, 60°C and 70°C respectively. Because the dissolution process is very fast and the temperature drops less than 1.5°C according to the test, it is unnecessary to heat the cell during the dissolution process and each temperature used for dissolution experiment can be considered as a constant. Besides the deionized water with different temperature, the deionized water is also prepared by mixing with standard pH buffer solution to obtain different pH. The standard pH buffer solutions used in this work are PHA-4 and PHA-10 buffer purchased from OMEGA. After adjusting the amount of pH buffer solution, the deionized water can show as different pH as 4, 7, 8, 9 and 10 respectively. These prepared deionized water with different pH are also used for the dissolution experiments in this work.

## 4. Mathematical model

### 4.1 Surface reaction model

Surface reaction model assumes that the dissolution rate is proportional to the particle surface area and the dissolution process is not controlled by the mass transport of dissolved solute but rather depended on the chemical reaction on particle surface. In this way the chemical reaction on the particle surface can be considered as the limiting step of the dissolution process[12].

Normally the dissolution rate is expressed as Eq. (1).

$$\frac{dC}{dt}V = K_r A \quad \text{Eq. (1)}$$

where  $K_r$  is the dissolution rate constant of surface reaction model,  $A$  is the surface area of spherical particle,  $C$  is the concentration of dissolved solute. Because the shape and density of sodium carbonate particle is assumed as the constant during the dissolution process, the real-time surface area of the particle can be calculated with Eq. (2).

$$A = A_0 \left( \frac{M}{M_0} \right)^{2/3} \quad \text{Eq. (2)}$$

where  $A_0$  is the initial surface area of particle,  $M_0$  is the initial mass of particle and  $M$  is the mass of undissolved particle.

As the density of sodium carbonate is a constant in this work, the mass of undissolved particle is thus converted with the real-time concentration and initial concentration of sodium carbonate in solvent which is shown as Eq. (3).

$$M = M_0 - (C - C_0)V \quad \text{Eq. (3)}$$

where  $C_0$  is the initial concentration of sodium carbonate which always equals to 0 in this work and  $V$  is the volume of solution.

Substituting the real-time surface area of particle with Eq. (2) and Eq. (3), Eq. (1) is transformed into Eq. (4)

$$\frac{dC}{dt}V = KA_0(1 - \frac{V}{M_0}C)^{2/3} \quad \text{Eq. (4) After}$$

integrating Eq. (4) with  $t=0$  and  $C=0$  at the starting point of dissolution process, Eq. (5) is obtained and used as the fitting equation to obtain the dissolution rate constant of surface reaction model.

$$C = \frac{M_0}{V} [1 + (\frac{A_0}{3M_0} Kt - 1)^3] \quad \text{Eq. (5)}$$

#### 4.2 Mass transport model

Based on the expression of dissolution rate shown in Eq. (1), the mass transport model takes into account the diffusion of dissolved sodium carbonate from particle surface into solvent and this diffusion is considered as the limiting step of dissolution process. This diffusion process is determined by the concentration difference of sodium carbonate between the concentration of sodium carbonate on particle surface and the concentration of sodium carbonate in solvent. The diffusion is also assumed to be one dimensional through a diffusion layer with a constant thickness. In this way, the dissolution rate of mass transport model can be expressed as Eq. (6)

$$\frac{dC}{dt}V = K_m A(C_{sat} - C) \quad \text{Eq. (6)}$$

where  $K_m$  is the dissolution rate constant of mass transport model;  $C_{sat}$  is the concentration of dissolved solute on particle surface which is assumed to be equal with the saturation of sodium carbonate in water.

After substituting Eq. (2) and Eq. (3) into Eq. (6), the dissolution rate can be transformed into Eq. (7)

$$\frac{dC}{dt}V = K_m A_0(C_{sat} - C)(1 - \frac{V}{M_0}C)^{2/3} \quad \text{Eq. (7)}$$

With the integration of  $C = 0$  when  $t = 0$  at starting point of dissolution process, the equation of mass transport model is shown as Eq. (8) and then used as the fitting model to obtain the dissolution rate constant of mass transport model.

$$K_m t = f(C) = \frac{Vx^2}{A_0 y^2} [0.5 \ln \frac{(x+y)^2}{y^2 - xy + x^2} + \sqrt{3} \tan^{-1} \frac{2x-y}{\sqrt{3}y} - 0.5 \ln \frac{(y+z)^2}{y^2 - yz + z^2} - \sqrt{3} \tan^{-1} \frac{2z-y}{\sqrt{3}y}] \quad \text{Eq. (8)}$$

Where  $x = (C - \frac{M_0}{V})^{1/3}$ ;  $y = (\frac{M_0}{V} - C_{sat})^{1/3}$ ;  $z = (-\frac{M_0}{V})^{1/3}$

### 5. Results and discussions

According to the auto-saved images of dissolution process, the diameter of sodium carbonate particle is measured for each dissolution experiment. An example of the diameter measurement of sodium carbonate particle dissolving at 30°C is shown in Fig.3. With the diameter measurement shown in Fig.3, it is clearly shown the diameter of this spherical sodium carbonate particle diminishes gradually with dissolution time. To obtain an accurate value of particle diameter at different dissolution time, a conception of particle diameter

for measurement in this work requires to be defined and discussed. Normally the diameter of a spherical or spherical-like particle for measurement can be considered as either the diameter of largest inscribed circle ( $D_i$ ) of particle or the diameter of smallest circumscribed circle ( $D$ ). In this work, the percentage of difference between smallest circumscribed circle diameter minus the largest inscribed circle over smallest circumscribed circle diameter,  $(D - D_i) / D$ , is always lower than 5% and this percentage of difference also decreases with dissolution time for every measurement. In this way the smallest circumscribed circle diameter of particle can be considered as the appropriate measured diameter in this work. Besides the determination of appropriate measured diameter, the measurement error of particle diameter also is caused by the resolution of image and the scale bar partially. The error comes from the measurement instrument systematically, however it is equivalent for every measurement and the value of error is negligible for the quantification of diameter. Therefore, it is convincing that the diameter of particle in this work can be measured accurately with the measurement of smallest circumscribed circle of each tested sodium carbonate particle and the value of measured particle diameter for each case is credible.

Based on the same measurement method shown above, the measured diameter of each sodium carbonate particle dissolving at each temperature and pH is plotted against dissolution time respectively. The results are shown in Fig.4 and Fig.5. For the measurement of particle diameter, when the diameter of particle is small enough the particle will be disaggregate into several irregular parts and dissolve very soon within only few seconds. Under this situation, it is very difficult to define and quantify the size once the particle starts disaggregation, and it is not precise to just insert 0 at the end of each plot of diameter. Therefore, that means the last point of each diameter plot is the last time that also can define and measure the remaining particle as spheres. It can be noticed that for all tested particles, the diameter of final point of each particle is similar to be approximately 0.3mm. Therefore, it can be confirmed that the phenomenon of sodium carbonate diminishing is trustable and the measurement is repeatable.

With the measured diameter shown in Fig.4 and Fig.5, the concentration of sodium carbonate in solution can be calculated with Eq. (9). The calculated concentrations of sodium carbonate at each temperature and pH are then plotted against dissolution time. The results of calculated concentration of dissolved sodium carbonate are shown in Fig.6 and Fig.7.

$$C = M_0 \left( \frac{D}{D_0} \right)^3 / V_0 \quad \text{Eq. (9)}$$

where  $C$  is the concentration of sodium carbonate in solvent,  $M_0$  is the initial mass of particle,  $D_0$  is the initial diameter of particle which always equals to 1.5mm,  $D$  is the real-time diameter of particle based on the values shown in Fig.4 and Fig.5,  $V_0$  is the volume of solvent.

In this work, the concentration of dissolved particle is based on the diameter of remaining particle. But it should be noticed that even if the diameter of particle is very difficult to define and measure after the disaggregation of the particle, the particle will finally dissolve completely in few seconds after disaggregation. So it can be confirmed that the concentration of sodium

carbonate in solvent will reach final maximum level at the end. As it is explained that the dissolving phenomenon after disaggregation is so quick within few seconds, the concentration will therefore reach the final level at the next point just after the last point of diameter plot and the concentration will keep stable in the next seconds or hours because the principle of this work is based on the visual particle measurement of the particle and the disappearing of the particle is regarded as the completing of the dissolution process. The plots of concentration also confirmed this process over their time scale.

According to the results shown in Fig.6 and Fig.7, the dissolution rate constant of each case is then quantified by fitting with surface reaction model and mass transport model separately. Based on surface reaction model, the concentration of dissolved sodium carbonate in solvent is fitted against dissolution time with Eq. (5). The fitting results with surface reaction model are shown in Fig. 8 and Fig. 9. Based on mass transport model,  $f(C)$  is fitted with against dissolution time Eq. (8). The fitting results with mass transport model are shown in Fig. 10 and Fig.11.

According to the fitting results shown in Fig.8 and Fig. 10, the adjusted correlation coefficient values ( $R^2$ ) shown in Fig. 10 are greater than the values shown in Fig. 8 at all temperatures. The adjusted correlation coefficient values shown in Fig. 10 are also high enough to suggest that the dissolution of single sodium carbonate particle with a increasing temperature is the mass transport controlled process where the diffusion of sodium carbonate from the particle surface into the solvent is the limiting step of this process, and the concentration difference between particle surface with the solvent is the driving force for the mass transport process of sodium carbonate.

Meanwhile, the adjusted correlation coefficient values shown in Fig. 9 and Fig. 11 are both high enough to suggest the proper dissolution mechanism. Although the values from mass transport model are slightly higher than those from surface reaction model, it is also speculated that the dissolution process of single sodium carbonate particle at an increasing pH is controlled by both surface reaction process and mass transport process where the limiting steps are both the chemical reaction of dissolution at particle surface and also the diffusion of dissolved sodium carbonate traveling from particle surface into solvent.

In this way, the dissolution rate constants of single sodium carbonate particle at different temperature and pH are quantified and the results are shown in Table 1 and Table 2 respectively. According to the results shown in Table 1 and Table 2, the dissolution rate constant apparently increases with temperature but decreases with pH significantly.

According to the results shown in Table 1, the dissolution rate constant apparently increases with temperature. The standard error also increases with temperature but the values are negligible to affect the conclusions. As the rate constant values shown in Table 1 obtained from the fitting with mass transport model, this increasing rate constant is caused by the diffusion enhancement with the increasing temperature. Theoretically speaking, the diffusion coefficient can be interpreted with Einstein-Stokes equation that is expressed as Eq. (9).

$$D_{\text{eff}} = \frac{K_B T}{6\pi\alpha\mu} \quad \text{Eq. (9)}$$

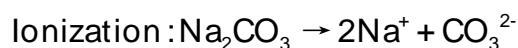


where  $K_B$  is Boltzmann's constant,  $T$  is the absolute temperature,  $\alpha$  is the radius of spherical particle and  $\mu$  is the kinematic viscosity of the medium.

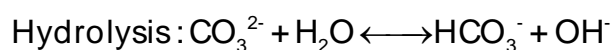
For a specific experimental temperature in this work, the parameters of Boltzmann's constant, radius of sodium carbonate granule are constant and only the parameters of absolute temperature and viscosity of solution are variables. Therefore, the changes of absolute temperature and viscosity of the solvent with temperature are the decisive parameters to determine the change of diffusion coefficient with temperature. According to the reference viscosity of water over temperature 30°C-70°C shown in Table 3[13] and the accepted value of Boltzmann constant in SI units which is  $1.37 \times 10^{-23} \text{ J} \cdot \text{K}^{-1}$ [14], the diffusion coefficient over different tested temperatures are calculated and the results are shown in Fig. 12. According to Fig. 12, it is clearly confirmed that the diffusion coefficient will increase with temperature increasing consequently. A higher diffusion coefficient normally reflects the quicker diffusion speed and process. Because the dissolution process of single sodium carbonate particle at the increasing temperature is controlled by the mass transport process, also known as a diffusion process, the dissolution rate constant of increasing with temperature therefore becomes an inevitable. This conclusion confirms the consequence of temperature's effect on dissolution kinetics from other previous works although these works target at other different materials with various methods for example Wang and Li's work on dissolution kinetics of granular calcium carbonate at 110-130°C[15] and Li *et al.*'s work on dissolution behavior of sodium titanate in sodium aluminate solutions at 180-240°C[16].

According to the results shown in Table 2, the dissolution rate constant from either surface reaction model or mass transport model decreases with the increasing of pH. As it is understood that the mass transport and diffusion process of sodium carbonate particle depends on the temperature's effect. For the circumstance of same temperature, the mass transport process is hardly impacted due to the same diffusion coefficient at same temperature. Therefore, the decreasing of dissolution rate constant with the increasing pH in this work is confirmed to rely on the surface reaction process and the chemical reaction at particle surface is the decisive step for the dissolution of sodium carbonate particle at an increasing pH.

For a typical chemical reaction of sodium carbonate in water at particle surface, it not only includes the ionization of sodium carbonate into sodium ions and carbonate ions, but also involves the possible hydrolysis reaction of ionized carbonate ions with  $\text{H}_2\text{O}$ . This hydrolysis reaction is the process of carbonate ions reacting with hydrogen ions to form bicarbonate ions and hydroxide ions. The hydrolysis reaction of carbonate ions is reversible and the equilibrium is sensitive. The formula of ionization and hydrolysis reaction is shown in Eq (10). Although the amount of ionized hydrogen ions in water is very low, the hydrolysis reaction also leads the dissolved sodium carbonate solution to weak alkaline. The increasing pH is usually understood as the increasing of hydroxide ions, therefore the chemical equilibrium of hydrolysis reaction will be broken and an unfavorable direction of chemical reaction happens to inhibit the hydrolysis reaction and also ionization reaction of sodium carbonate. In this way, the increasing pH is confirmed to weaken the surface chemical reaction of sodium carbonate and the dissolution process is also reduced because it is controlled by the surface chemical reaction.



Eq(10)



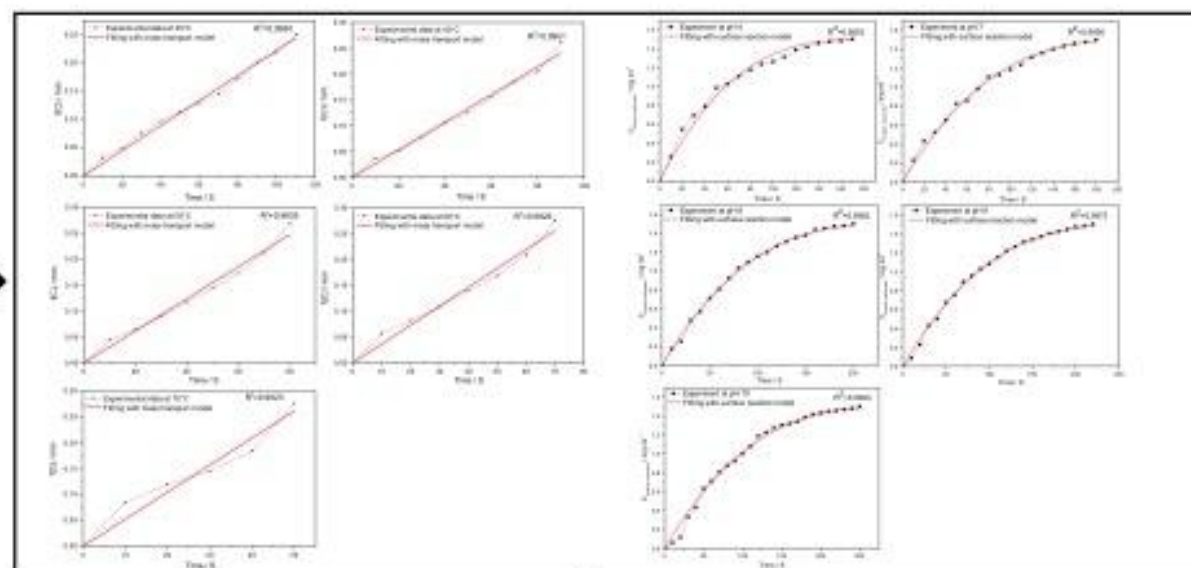
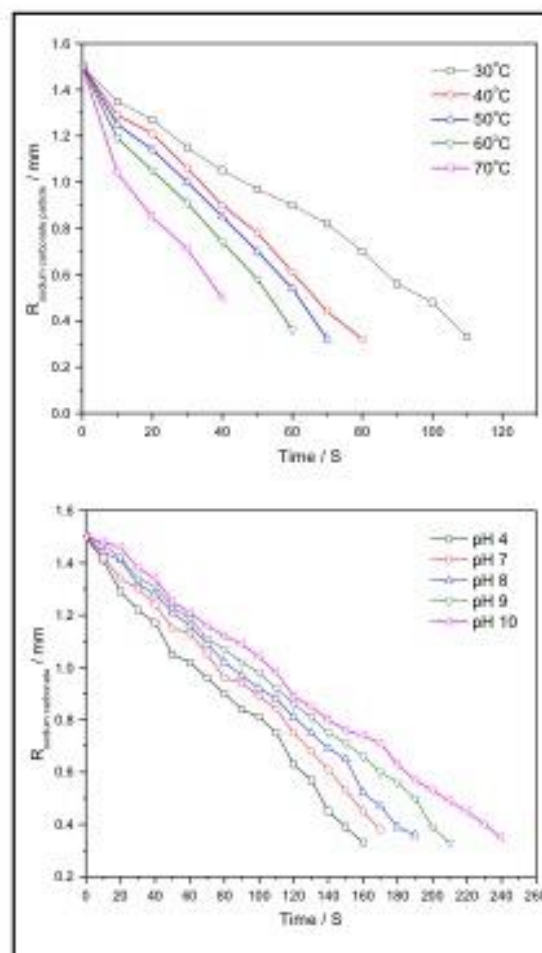
## 6. Conclusions

Dissolution kinetics of single sodium carbonate particle is investigated successfully in this work with image analysis method. Image analysis method is well applied into the measurement of dissolution process of single sodium carbonate particle, and both surface reaction model and mass transport model are successfully implemented as the mathematical model to evaluate the dissolution mechanism and quantify the dissolution rate constant. According to the fitting results with both two dissolution models, it is confirmed that the dissolution process of single sodium carbonate particle at a fixed pH but increasing temperature is controlled by the mass transport (diffusion) of dissolved sodium carbonate from particle surface into solvent. The dissolution process at a fixed temperature but increasing pH is controlled by the chemical reaction of sodium carbonate with water at particle surface. In this way with the increasing temperature, the dissolution rate constant of mass transport model is quantified to increase with temperature because of the diffusion enhancement with the temperature increasing. With the increasing pH, the dissolution rate constant of surface reaction model is also quantified to decrease with pH because of the weakness of chemical reaction of sodium carbonate at the experimental condition of increasing pH.

## Acknowledgements

I would like to thank the Institute of Particle and Science Engineering, University of Leeds and Procter & Gamble Newcastle Innovation Centre (UK) for partially funding the project.

## Graphical abstract



| Temp. / °C | Dissolution rate constant (Mass transport model)<br>$K_{ms} / \text{mm S}^{-1}$ | pH | Dissolution rate constant (Mass transport model)<br>$K_{ms} / \text{mm S}^{-1}$ | Dissolution rate constant (Surface reaction model)<br>$K_{sr} / \text{mg mm}^{-2} \text{S}^{-1}$ |
|------------|---|----|---|--|
| 30         | 0.0022  | 4  | 0.0015  | 0.00067  |
| 40         | 0.0027  | 7  | 0.0013  | 0.00055  |
| 50         | 0.0031  | 8  | 0.0012  | 0.00049  |
| 60         | 0.0037  | 9  | 0.0011  | 0.00045  |
| 70         | 0.0052  | 10 | 0.00084   | 0.00040  |

## Abstract

Dissolution kinetics of sodium carbonate is investigated with the image analysis method at the approach of single particle. The dissolution experiments are carried out in an aqueous solution under a series of controlled temperature and pH. The selected sodium carbonate particles are all spherical with the same mass and diameter. The dissolution process is quantified with the measurement of particle diameter from dissolution images. The concentration of dissolved sodium carbonate in solvent is calculated with the measured diameter of particle. Both surface reaction model and mass transport model are implemented to determine the dissolution mechanism and quantify the dissolution rate constant at each experimental condition. According to the fitting results with both two models, it is clarified that the dissolution process at the increasing temperature is controlled by the mass transport of dissolved sodium carbonate travelling from particle surface into solvent. The dissolution process at the increasing pH is controlled by the chemical reaction on particle surface. Furthermore, the dissolution rate constant for each single spherical sodium carbonate particle is quantified and the results show that the dissolution rate constant of single spherical sodium carbonate increases significantly with the rising of temperature, but decreases with the increasing of pH conversely.

## References

- [1] W. I. Higuchi, Diffusional models useful in biopharmaceutics: Drug release rate processes. *J. Phar. Sci.* 56 (3) (1967) 315-324.
- [2] J. Philibert. One and a half century of diffusion: Fick, Einstein, before and beyond. *Diffu. Fundam.* 2(1) (2005) 1-10.
- [3] A.A. Noyes, W.R. Whitney. The rate of solution of solid substances in their own solutions. *J. Amer. Chem. Soc.* 19 (12) (1897) 930-934.
- [4] A.W. Hixson, J.H. Crowell. Dependence of reaction velocity upon surface and agitation. *Ind. Eng. Chem.* 23 (10) (1931) 1160-1168.
- [5] M. Dali. Determination of mass transfer dissolution rate constants from critical time of dissolution of a powder sample. *Phar. Dev. and technol.* 4 (1) (1999) 1-8.
- [6] S.V. Dorozhkin. Fundamentals of the wet-process phosphoric acid production: 1. Kinetics and mechanism of the phosphate rock dissolution. *Ind. Eng. Chem. Res.* 35 (11) (1996) 4328-4335.
- [7] S.L. Raghavan, R.I. Ristic, D.B. Sheen, J.N. Sherwood. Dissolution kinetics of single crystals of  $\alpha$ -lactose monohydrate. *J. Phar. Sci.* 91 (10) (2002) 2166-2174.
- [8] F. Štěpánek. Computer-aided product design: granule dissolution. *Chem. Eng. Res. Des.* 82 (11) (2004) 1458-1466.
- [9] J. Swarbrick, D. Ma. In vitro dissolution of dapsone. *J. Phar. Pharm.* 33 (1) (1981) 787-789.
- [10] D.E. Wurster, P.W. Taylor. Dissolution rates. *J. Pharm Sci.* 54 (2) (1965) 169-175.
- [11] N.A. Riley. Projection sphericity. *J. Sed. Res.* 11 (2) (1941) 94-95.
- [12] R.G. Haverkamp, B.J. Welch. Modelling the dissolution of alumina powder

in cryolite. *Chem. Eng. Process.* 37 (2) (1998) 177-187.

[13] L.Korson, W.Drost-Hansen, F.J.Millero. Viscosity of water at various temperatures. *J. Phys. Chem.* 73 (1) (1969) 34-39.

[14] W. Lopes. Boltzmann's constant. *Revista Brasileira de Ensino de Fisica.* 32 (3) (2010) 1-4.

[15] T. Wang, Z. Li. Dissolution kinetics of granular calcium carbonate in concentrated aqueous sodium dichromate solution at pH 6.0-7.0 and 110-130°C. *J.Colloid Interface Sci.* 281 (2005) 130-135.

[16] X.Li, S. Yu et al. Dissolution behaviour of sodium titanate in sodium aluminate solutions at elevated temperatures. *Hydrometallurgy.* 147-148 (2014) 73-78.

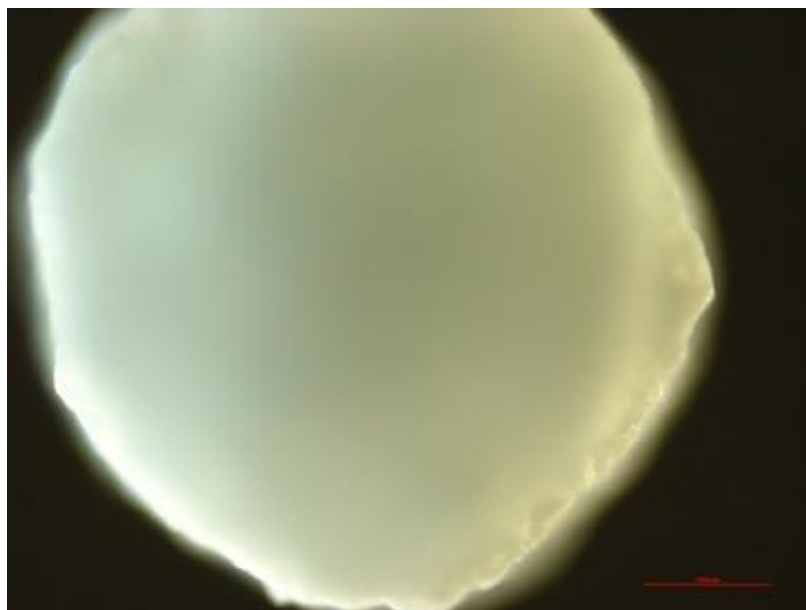


Fig.1. Spherical sodium carbonate particle into dissolution experiment

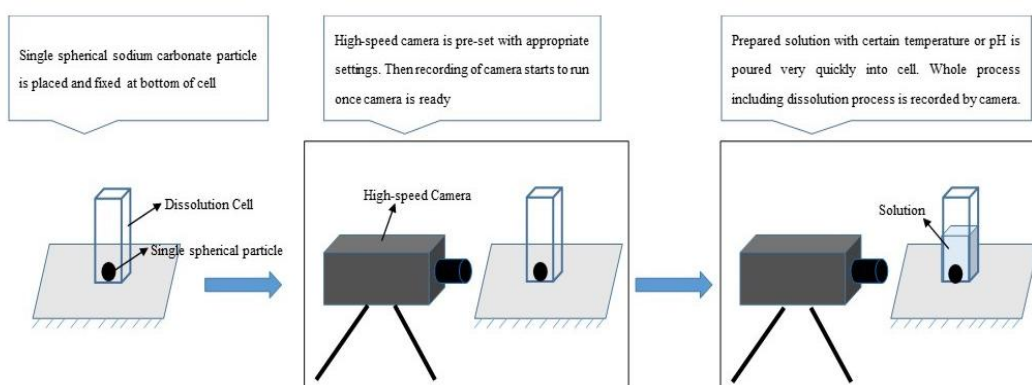


Fig.2. Scheme of a typical dissolution experiment

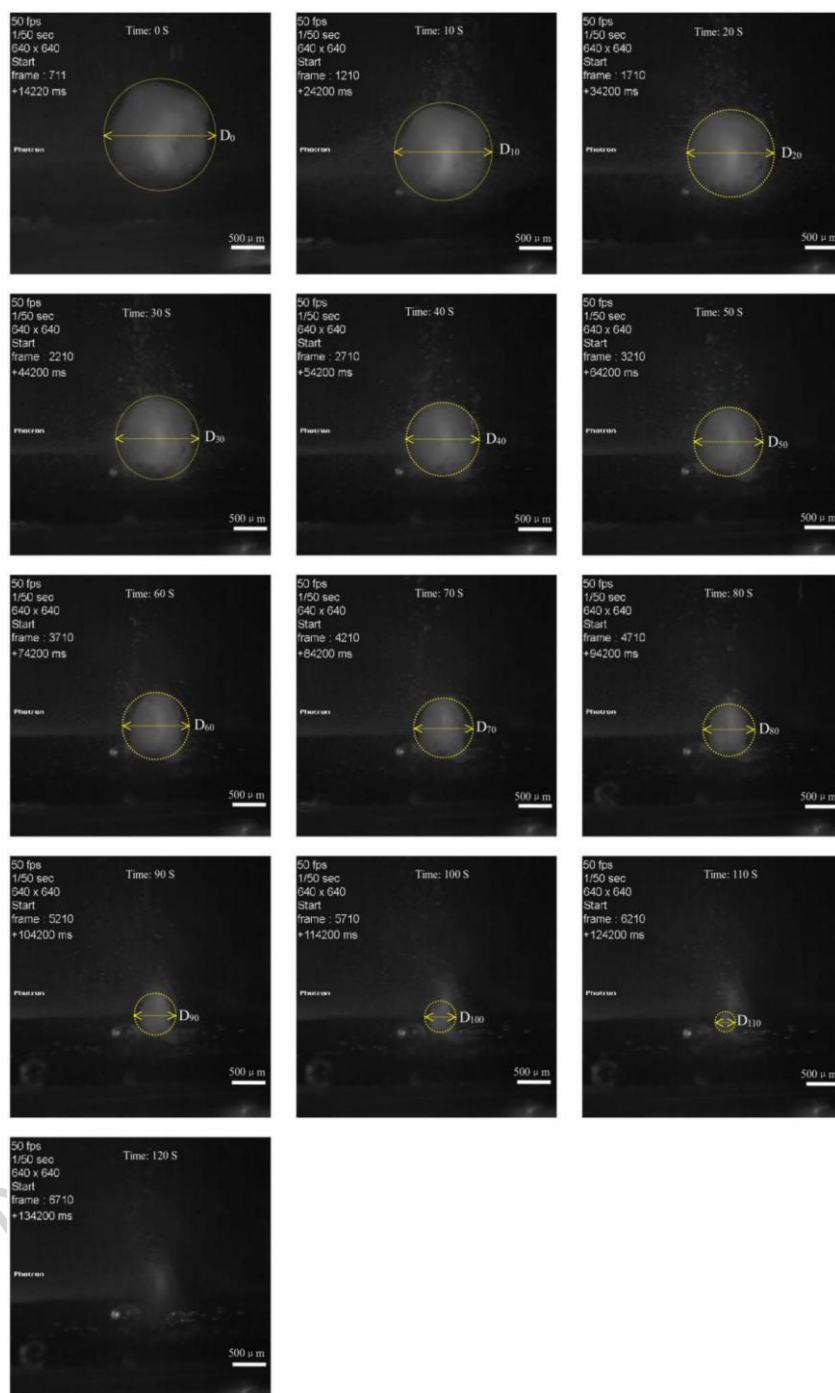


Fig.3. Diameter measurement of sodium carbonate particle dissolving at 30°C

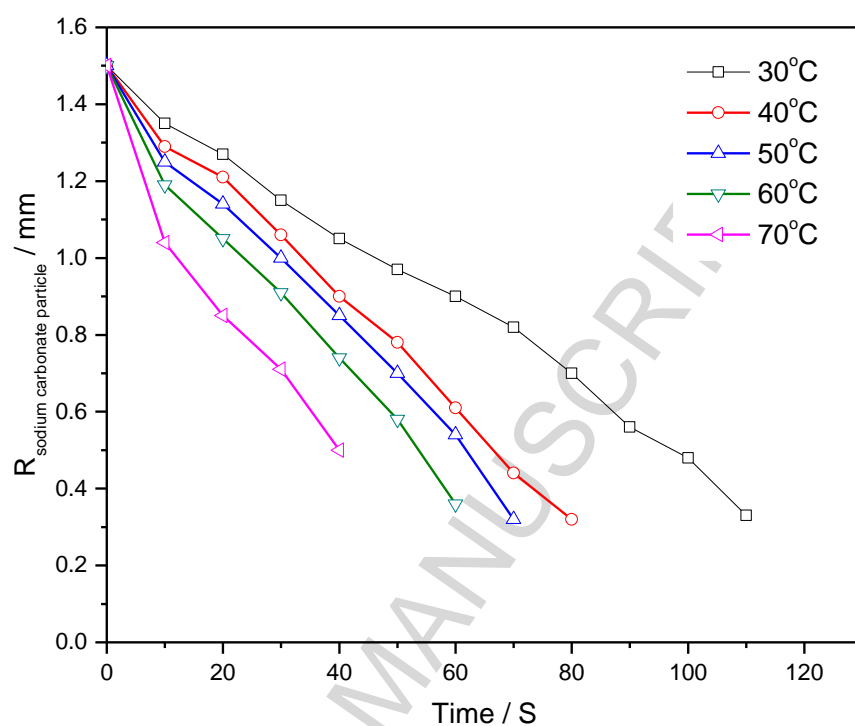


Fig.4. Measured diameter of sodium carbonate particle dissolving at different temperature

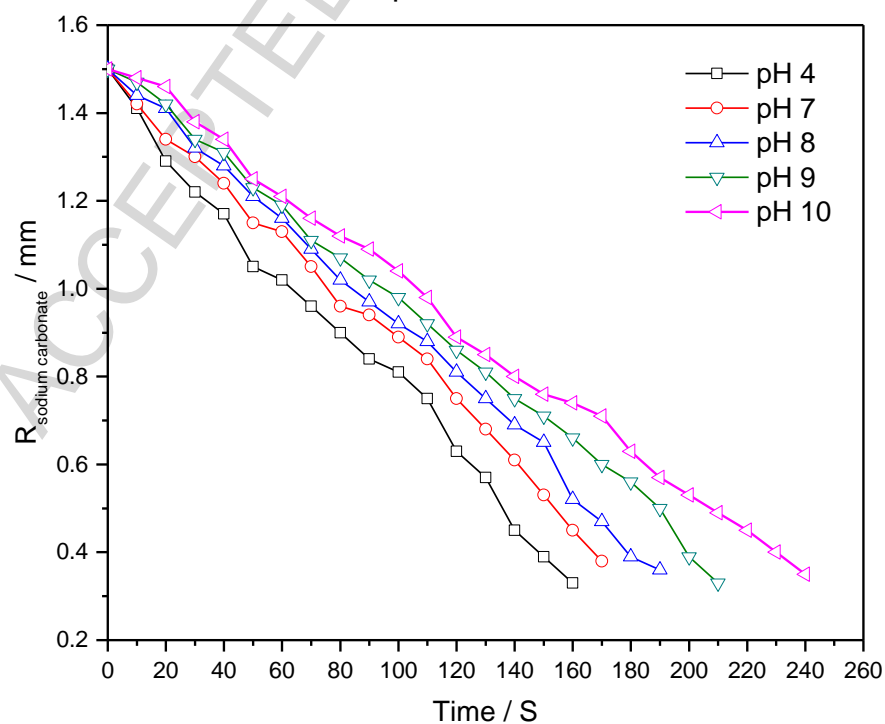


Fig.5. Measured diameter of sodium carbonate particle dissolving at different pH



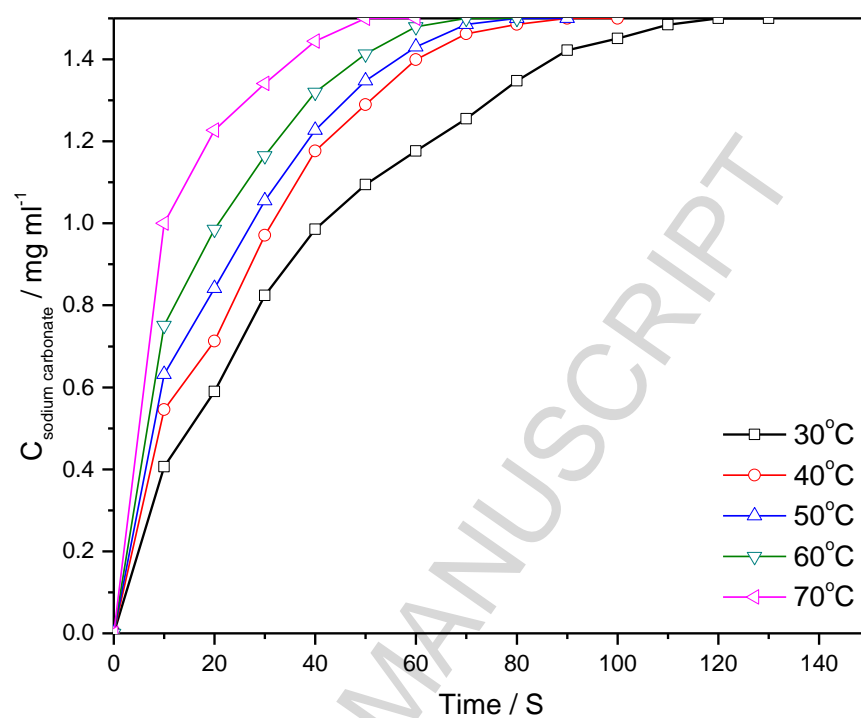


Fig.6. Concentration of dissolved sodium carbonate at different temperature

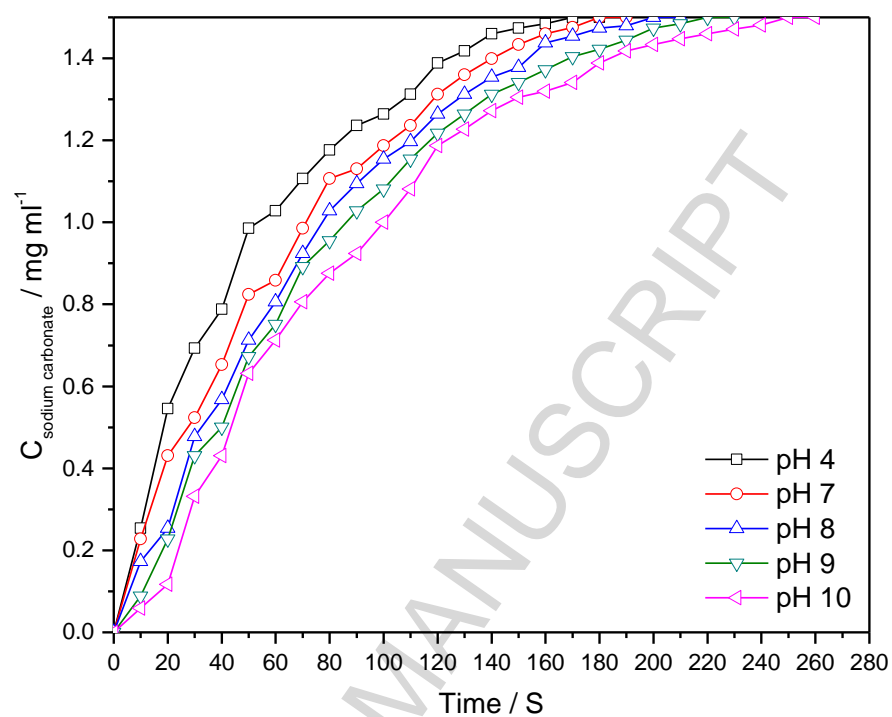


Fig.7. Concentration of dissolved sodium carbonate at different pH

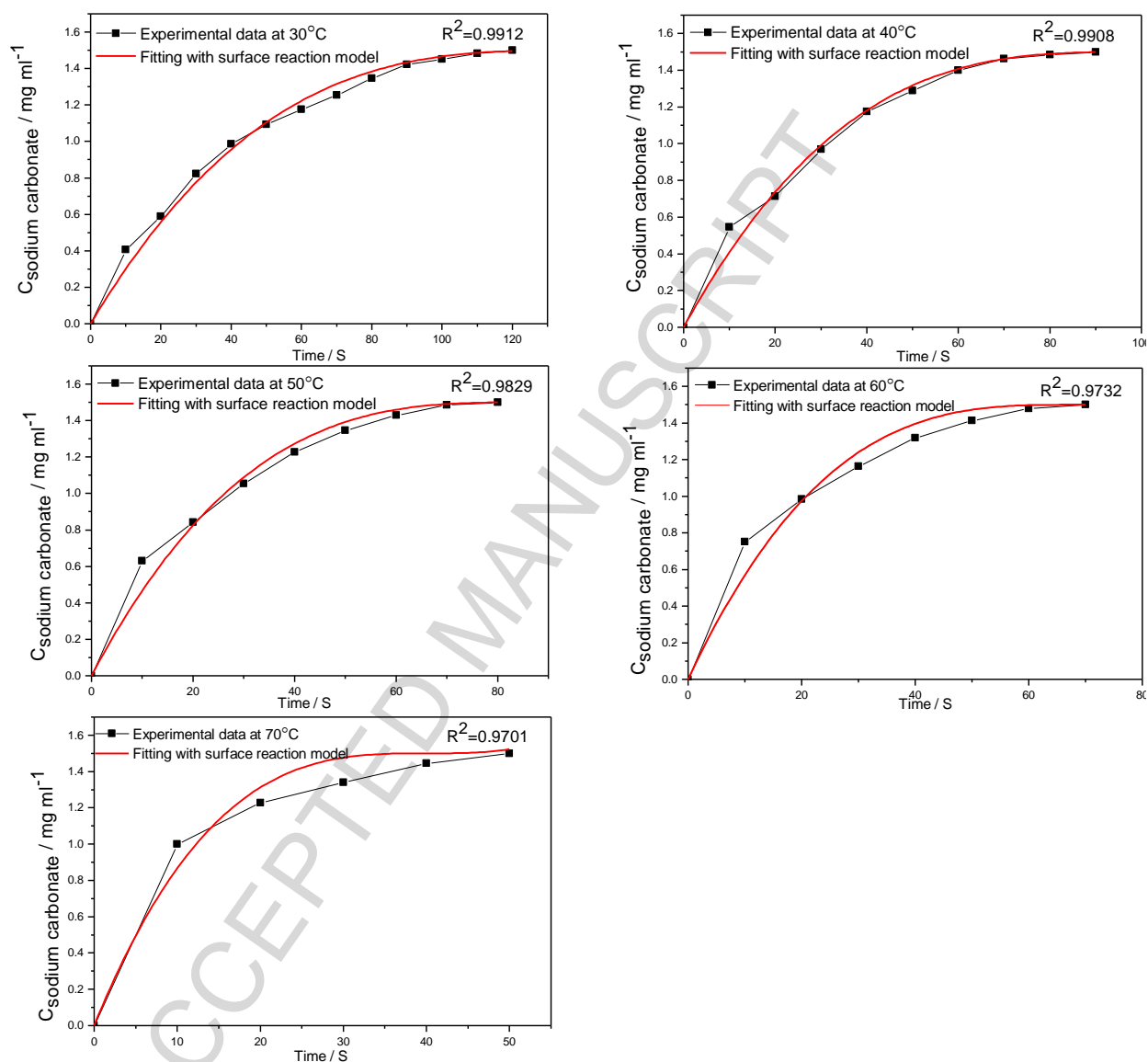


Fig.8. Fitting with surface reaction model for the dissolution experiment at 30°C / 40°C / 50°C / 60°C / 70°C

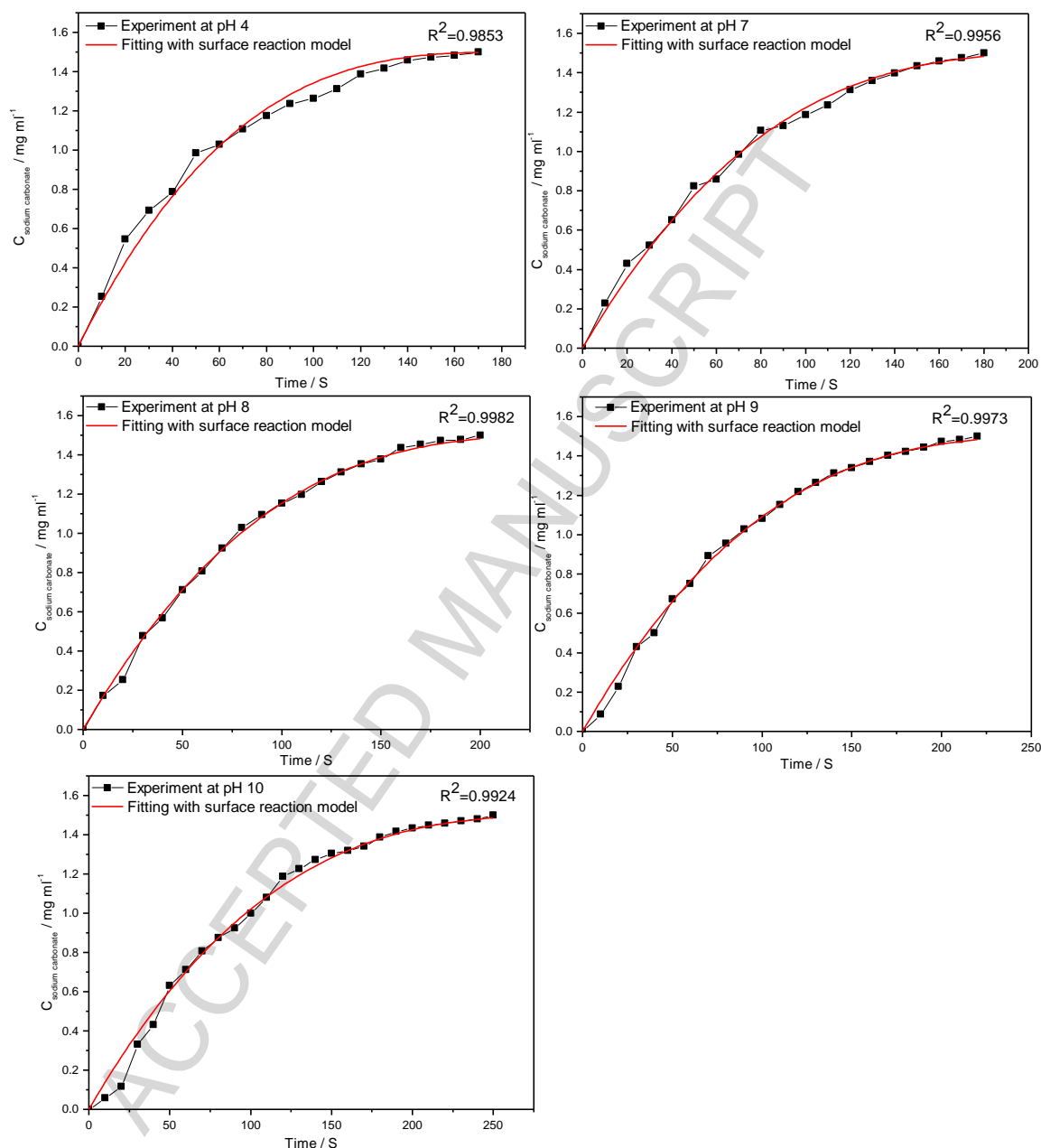


Fig.9. Fitting with surface reaction model for the dissolution experiment at pH 4 / 7 / 8 / 9 / 10

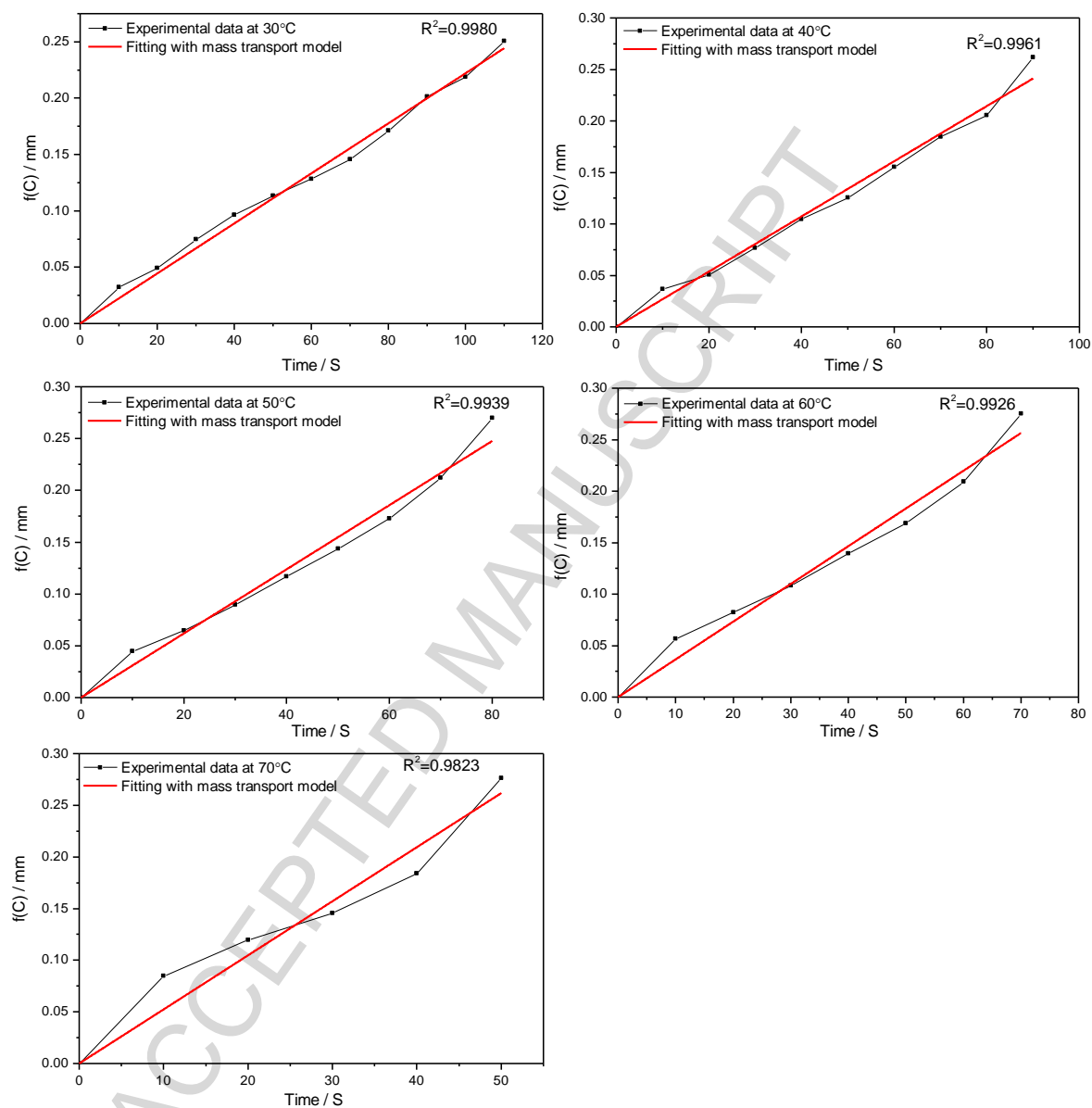


Fig.10. Fitting with mass transport model for the dissolution experiment at 30°C / 40°C / 50°C / 60°C / 70°C

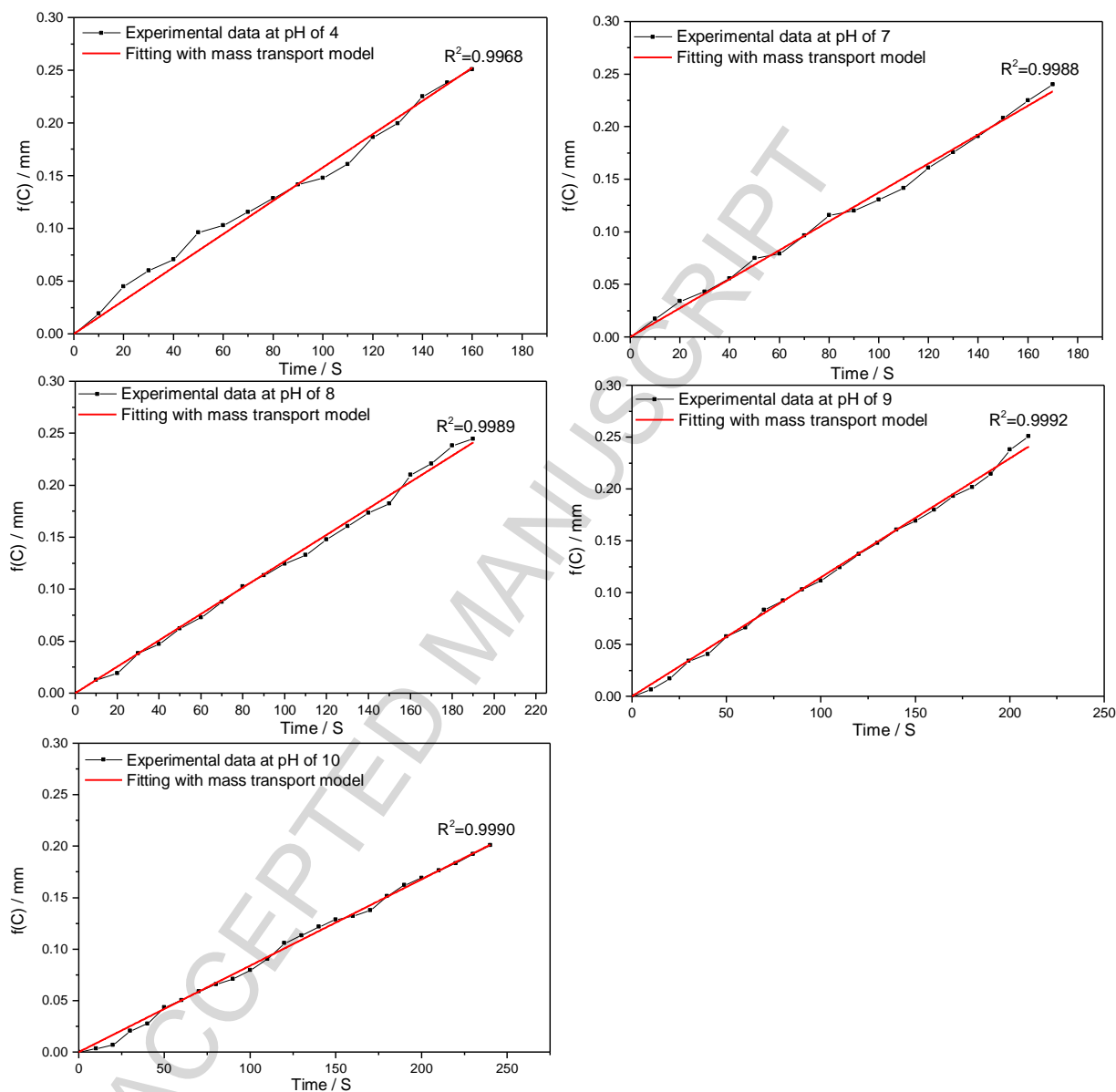


Fig.11. Fitting with mass transport model for the dissolution experiment at pH 4 / 7 / 8 / 9 / 10

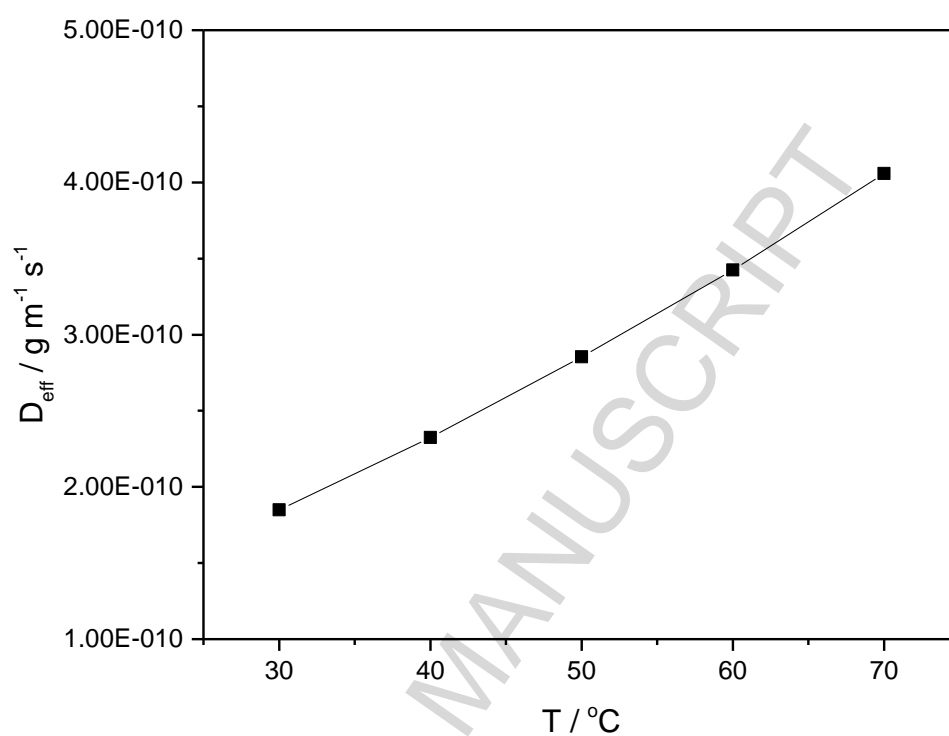


Fig.12 Diffusion coefficient of sodium carbonate particle over different dissolution temperature

Table 1. Dissolution rate constant  $K_m$  at different temperature

| Temp. / °C | Dissolution rate constant (Mass transport model)<br>$K_m / \text{mm}\cdot\text{s}^{-1}$ | Standard error        |
|------------|---|-----------------------|
| 30         | 0.0022  | $2.90 \times 10^{-5}$ |
| 40         | 0.0027  | $5.33 \times 10^{-5}$ |
| 50         | 0.0031  | $8.08 \times 10^{-5}$ |
| 60         | 0.0037  | $1.12 \times 10^{-4}$ |
| 70         | 0.0052  | $2.86 \times 10^{-4}$ |



Table 2. Dissolution rate constant  $K_m/K_r$  at different pH

| pH | Dissolution rate constant (Mass transport model)<br>$K_m / \text{mm} \cdot \text{s}^{-1}$ | Standard error        | Dissolution rate constant (Surface reaction model)<br>$K_r / \text{mg} \cdot \text{mm}^{-2} \cdot \text{s}^{-1}$ | Standard error        |
|----|---|-----------------------|--|-----------------------|
| 4  | 0.0015  | $2.18 \times 10^{-5}$ | 0.00067  | $1.90 \times 10^{-5}$ |
| 7  | 0.0013  | $1.15 \times 10^{-5}$ | 0.00055  | $7.88 \times 10^{-6}$ |
| 8  | 0.0012  | $9.45 \times 10^{-6}$ | 0.00049  | $4.44 \times 10^{-6}$ |
| 9  | 0.0011  | $7.15 \times 10^{-6}$ | 0.00045  | $4.77 \times 10^{-6}$ |
| 10 | 0.00084   | $5.32 \times 10^{-6}$ | 0.00040  | $6.89 \times 10^{-6}$ |

Table 3. Viscosity of water from 30°C to 70°C

| Temperature /°C  | 30    | 40    | 50    | 60    | 70    |
|--|-------|-------|-------|-------|-------|
| Viscosity $\times 10^6 / \text{m}^2 \cdot \text{s}^{-1}$ | 0.801 | 0.658 | 0.553 | 0.475 | 0.413 |